Biomass Conversion and Biorefinery
https://doi.org/10.1007/s13399-022-03391-3

ORIGINAL ARTICLE

Investigation of static and dynamic mechanical properties of CPFLSF and PPLSFreinforced polyester hybrid composites

M. Jayaraj[1] · **Rama Thirumurugan**[2] · **D. Shanmugam**[3]

Received: 3 June 2022 / Revised: 6 October 2022 / Accepted: 10 October 2022

Abstract
The composites are prepared by reinforcing with 7-mm-short treated coconut tree primary flower leaf stalk fiber (CPFLSF) and palmyra palm leaf stalk fiber (PPLSF) in the polyester matrix. Compression molding was used to fabricate the hybrid composite plates. The 7C10P20C (treated 7-mm coconut tree primary flower leaf stalk fiber/palmyra palm leaf stalk–reinforced polymer hybrid composite) showed the maximum tensile strength (47.14MPa), flexural strength (73.56MPa), and impact strength (10.56kJ/m^2), respectively. Reinforcement of alkali-treated palmyra palm fibers enhanced the loss modulus, storage modulus, and damping factor (tanδ) for the 7C10P20C. The final thermal decomposition stage of the 7C10P20 hybrid composite takes place at 550°C with a maximum residual mass of 26%. The morphological study confirms the less pullout, fracture surface, and better bonding between the matrix and reinforcement of the 7C10P20C. A minimum amount of water was absorbed by the 7C10P20C during the water absorption test, due to the maximum hydrophobic nature. In the dynamic mechanical analysis (DMA), maximum storage modulus (E′) and loss modulus (E″) were observed in the values of 1392MPa and 259.2 MPa obtained for the 7C10P20 hybrid composite. The measured property results are compared with each other and with various natural fiber polymer composites and reported in this work. The results demonstrate that the produced composites are stable, with high tensile strength and bending rigidity, allowing material engineers to use the material in light-load applications.

Keywords Coconut tree primary flower leaf stalk fiber (CPFLSF) · Palmyra palm leaf stalk (PPLSF) morphological study · Tensile strength · Flexural strength · Impact strength · Water absorption test

1 Introduction

In recent years, maintaining the global green balance has played an important role and environmental awareness is increasing day by day. Today, researchers are looking for alternatives to natural fiber–filled polymer materials that are lower in environmental impact, cheaper, and reliable; have feasible excellent mechanical properties, minimal density, and high stiffness; and are harmless [1, 2]. Due to the excellent properties and cost ratio of unsaturated polyester, resins were used in many applications, such as sheet molding, bulk molding, and laser printer toners, which have good impact resistance, good wear resistance, good fatigue resistance, and higher stiffness temperature [3]. Many authors have documented the use of natural fibers such as banana, elephant grass, sisal, jute, vakka, bamboo, *Roystonea regia*, and coconut as reinforcement in composite materials [4]. Other than the commonly used natural fibers for reinforcement in polymer composites (kenaf, hemp, flax, ramie, bamboo, coir, bagasse, sugarcane) are finding applications in a variety of fields such as automotive, marine, sports, and structural [5–7]. In addition to that, the chemical treatment of natural fibers also improves the performance of composites. Among the chemical treatments, the alkali treatment is the most widely used natural fiber (such as alpha, bamboo, sisal, betel nut). Surface modification method and its reported that 6% NaOH treatment can improve the mechanical properties of sisal and

✉ M. Jayaraj
jayaraj.m21@gmail.com

Rama Thirumurugan
rama.thirumurugan@gmail.com

D. Shanmugam
dshanmugam@rediffmail.com

1 Department of Mechanical Engineering, P.A College of Engineering and Technology, Pollachi, India

2 Department of Mechanical Engineering, Dr. Mahalingam College of Engineering and Technology, Pollachi, India

3 Department of Automobile Engineering, Dr. Mahalingam College of Engineering and Technology, Pollachi, India

Published online: 18 October 2022

jute compounds [8]. Although there is a lot of literature on hybrid composites in the studies of banana/sisal, oil palm/jute fruit clusters, glass/sisal, and jute/coir fiber–reinforced hybrid composites, it has been proven that hybrids can provide good mechanical behavior [9]. There are several other case studies on the mechanical properties of coir fiber/glass, jute/basalt, jute/basalt/aluminum, and kevlar/jute [10, 11]. Based on these, it has been found that hybridization reduces the use of conventional synthetic fibers in a number of industrial applications to achieve desired properties [12]. The tensile strength of the hybrid composite (79.6 MPa) significantly increased with 15 wt% Jatropha Shell Powder loading of size 150–250 m as compared to epoxy glass fiber composite [13]. According to studies of various natural fiber composites. Rambans (Agave) fiber composite had maximum tensile strength found to be 95.27 MPa with 4.7 J/m^2 impact strength (35.7 MPa) [14]. Subsequently, with the addition of *Vigna mungo* powder, flexural and hardness properties were greatly improved [15]. Hemp/nettle-polyester hybrid composites with a higher weight percentage (9 wt%) showed the highest tensile (42.41 MPa), flexural (78.52 MPa), impact (22.72 kJ/m^2), and harder value (46.7 HV) among these materials [16].

Based on the above discussion, the objective of the present work is to study the effect of alkali-treated 7-mm-short coconut tree primary flower leaf stalk fiber (CPFLSF) and palmyra palm leaf stalk fiber (PPLSF) on the performance (static and dynamic mechanical, water, and thermal properties) of this polymer hybrid.

2 Materials and methods

2.1 Extraction of PPLSF and CPFLSF

The PPLSF were extracted from the leaf stalks of the palmyra palm tree (*Borassus flabellifer*) and CPFLSF were cut from the primary leaf stalk of the coconut tree (*Cocos nucifera* L.). Both leaf stalks' skin and edges of the thorns were manually shaved and retted in water for 40 days. Further to retting, the fibers were removed from the stalk by using a wooden hammer. The fibers were then cleaned, washed, and dried in sunlight for 1 day to remove moisture and other impurities from the surface [14]. The extracted fiber after the above processes is shown in Fig. 1.

Table 1 Physical properties of PPLSF and CPFLSF

S. No.	Physical properties	PPLSF	CPFLSF
1	Density (g/cm^3)	1.4	1.11
2	Diameter (μm)	150	79.08
3	Microfibril angle (degree)	7.19	8.15
4	Tensile strength (MPa)	276	265
5	Young's modulus (GPa)	3.24	2.75

2.2 Alkali treatment of fibers

Both CPFLSF and PPLSF were cleaned with water to remove impurities. The fibers were immersed in 6% of NaOH for 30 min [17]. Subsequently, the fibers were washed with distilled water several times and then immersed in very diluted HCL followed by cleaning with tap water and distilled water several times to remove the excess NaOH sticking to the fiber surface and they were finally dried at room temperature for 2 days [15]. The physical properties of PPLSF and CPFLSF are included in Table 1.

2.3 Fabrication of hybrid composite

The chemicals such as unsaturated polyester resin, methyl ethyl ketone peroxide (catalyst), and cobalt octoate (accelerator) are used for the fabrication of composite. Before the

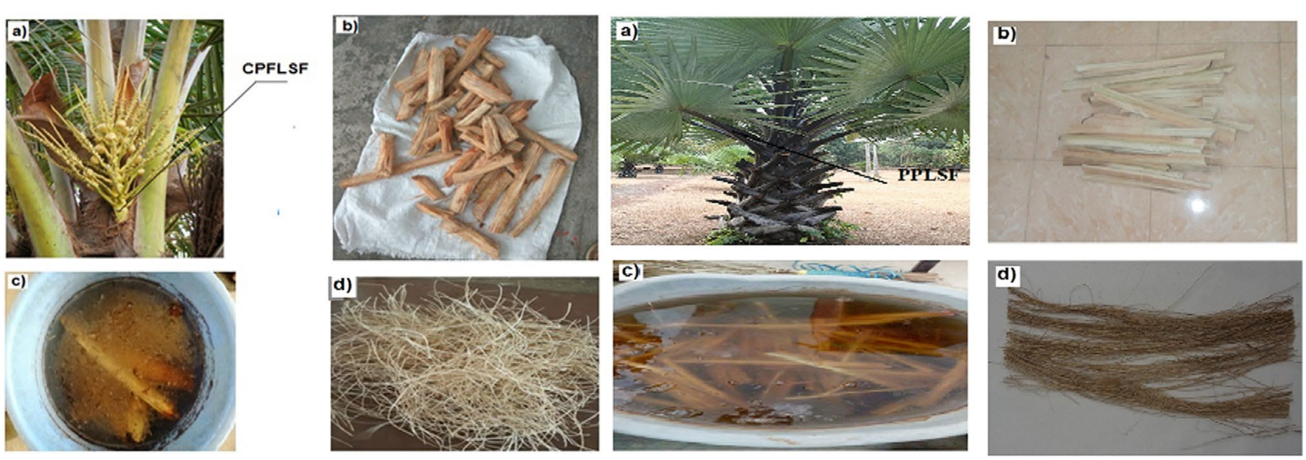

Fig. 1 Extraction of PPLSF and CPFLSF. **a**) Fiber parts' name. **b**) Leaf stalks. **c**) Retted fibers. **d**) Extracted fibers

preparation of the composite, the fibers were pressed by placing the fibers inside the die to form on a woven mat. The non-woven mat thus fabricated was placed inside the mold cavity and the prepared matrix was poured inside the mold and the die was closed and kept by applying a force of 1 ton by hydraulic compression to produce a hybrid composite [16]. The ratio of fiber and matrix was kept at 30:70 while fabricating all the composite plates. The prepared composite plates are shown in Fig. 2. Finally, the specimens were cut to the required size. The detail of the designation of CPFLSF/PPLSF hybrid polyester composites is given in Table 2.

2.4 Static mechanical test

Instron tensile tester was used for determining the tensile properties of the composites. ASTM: D638 (165 19 × 3 mm^3) standard was used for testing the composites for tensile properties with the crosshead speed of 5 mm/min. The flexural test for those specimens was conducted as per the ASTM D790-03 (127 × 12.7 × 3 mm^3), using Kalpak Universal Testing Machine with a capacity of 20kN and with a crosshead speed of 2mm per minute. The composite was cut into the specimens as per ASTM: D256 (164 × 13 × 3 mm^3) for impact test [18]. For all tests, three specimens were tested and average values were reported.

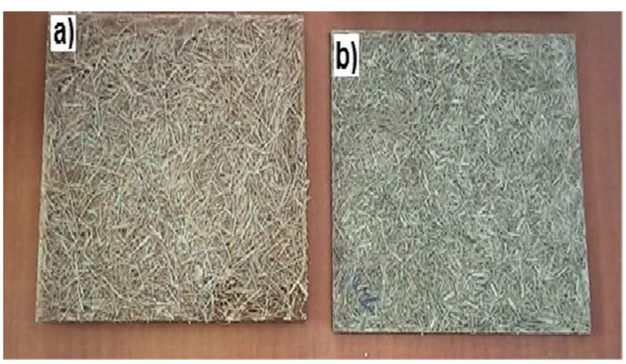

Fig. 2 Hybrid composite materials of **a**) 7C20P10C and **b**) 7C10P20C

2.5 Density and void fraction

The Archimedes principle was used to calculate the hybrid composite's actual density. This concept states that when a material is submerged in a liquid, the weight of the liquid it displaces is equal to the apparent reduction in the material weight. Distilled water was chosen as the testing medium. The ASTM standard D792 specifies this procedure. Using the following equation, the hybrid composite's true density was determined.

$$\rho a = \frac{\rho w Wa}{Wa - Ww} \tag{1}$$

where

ρa actual density of hybrid composite
ρw density of distilled water
Wa weight of the sample in air
Ww weight of the sample in water

The following equation, which was provided by Agarwal and Broutman, may be used to calculate the theoretical density (t) of the composite material.

$$\rho t = \frac{1}{\left(\frac{Wf}{\rho f}\right) + \left(\frac{Wm}{\rho m}\right)} \tag{2}$$

where
Wf weight fraction for fiber
Wm weight fraction for matrix
ρf density of fiber
ρm density of matrix

The following equation can be used to determine the volume percentage of voids.

$$Vv = \frac{(\rho t - \rho a)}{\rho t} \tag{3}$$

Table 2 Composition and designation of the hybrid polyester composite

Name of the fiber	Composite designation	Composition of PPLSF	Composition of CPFLSF	Composition of resin
Alkali-treated 7mm with 20 wt% coconut tree primary flower leaf stalk fiber (CPFLSF)/10 wt% palmyra palm leaf stalk fiber (PPLSF)–reinforced polyester hybrid composite	7C20P10C	10%	20%	70%
Alkali-treated 7mm with 10 wt% coconut tree primary flower leaf stalk fiber (CPFLSF)/20 wt% palmyra palm leaf stalk fiber (PPLSF)–reinforced polyester hybrid composite	7C10P20C	20%	10%	70%

where

ρt theoretical density of the hybrid composite
ρa actual density of the hybrid composite

2.6 Water absorption of composites

The specimens for the water absorption test were cut and the water absorption test was performed in accordance with ASTM D570 standards. At regular intervals of time, the immersed specimens were taken out and the weight was noted [19]. The percentage of water absorption in the composites was calculated by

$$\%WC = \frac{W_O - W_t}{W_O} \times 100 \tag{4}$$

where

W_C water absorption of the composites
W_o initial dry weight of the composites
W_t wet weight of the sample after a specific interval of time in the water

2.7 Dynamic mechanical analysis (DMA)

DMA was performed using SII (Inkarp) DMS 6100 make. A frequency of 1Hz and dual cantilever bending mode were used for the experiment. The specimen sizes of 50 mm × 50 mm × 3 mm were cut from the fabricated composite plates and the test was conducted at room temperature. A heating rate of 2°C/min is used during the test [20].

2.8 Thermogravimetric analysis (TGA) of composites

The thermal stability of the composites was determined using ASTM E 1131 standard. The weight of the specimen was analyzed by TGA/DTG using a PerkinElmer machine at a temperature range of 50–750°C at a heating rate of 10°C/min and 20 ml/min nitrogen atmosphere [14].

2.9 Scanning electron microscope (SEM) of composites

SEM was performed using SEM JEOL JSM 6390 at an accelerating voltage of 10KV. The surface morphology of the fractured surface of composite materials after tensile testing was examined using the machine [11].

3 Result and discussion

3.1 Tensile properties

Figures 3 and 4 illustrate the tensile strength and tensile modulus of the CPFLSF/PPLSF-reinforced polyester hybrid composites. The tensile strength of the composites increased with the increase of PPLSF weight percentage in the hybrid composite. As estimated, non-hybrid PPLSF–reinforced composites showed maximum tensile strength compared to the non-hybrid CPFLSF–reinforced composites. The non-hybrid PPLSF–reinforced composites showed a tensile strength of 45.13 MPa, which is 23.97% greater than the non-hybrid CPFLSF–reinforced composites. However, the 7C20P10C which had the maximum amount of CPFLSF exhibited a tensile strength of 40.24 MPa. It is decreased by 10.86%, compared to the non-hybrid PPLSF–reinforced composites. The 7C10P20C tensile strength is 47.14 MPa, which marginally increased by 4.26% compared to the non-hybrid PPLSF–reinforced composites.

Meanwhile, tensile modulus increased due to increased PPLSF content in reinforced hybrid composite. The maximum tensile modulus in the non-hybrid PPLSF–reinforced composites is 2.13GPa, whereas the non-hybrid CPFLSF–reinforced composite showed the lowest tensile modulus. The 7C10P20C showed a tensile modulus of 2.67GPa, which is higher by 26.21% and 20.21% of 7C20P10C and the non-hybrid PPLSF–reinforced composite, respectively.

Due to the higher mechanical properties of PPLSF over CPFLSF, the combination of PPLSF in the composites is helpful to improve the tensile properties of the hybrid composites. This can be attributed to the optimum L/D ratio and stiffness of PPLSF, which leads to improvement in the tensile strength of the hybrid reinforced composite. When

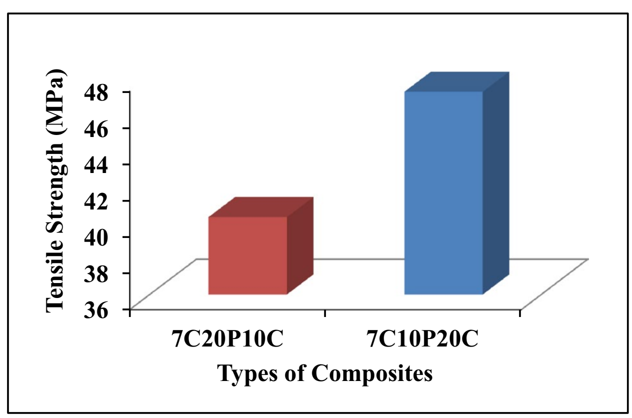

Fig. 3 Tensile strength of CPFLSF/PPLSF hybrid–reinforced composites

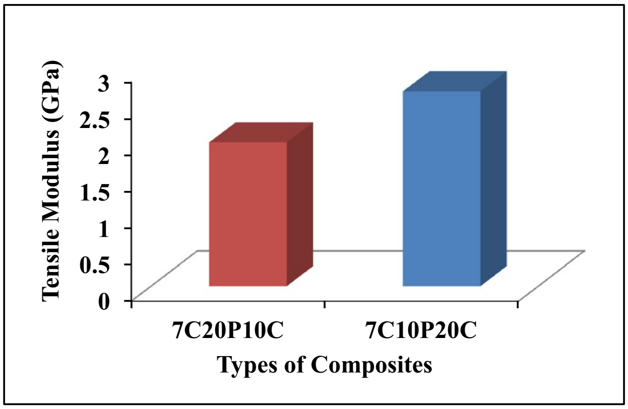

Fig. 4 Tensile modulus of CPFLSF/PPLSF hybrid–reinforced composites

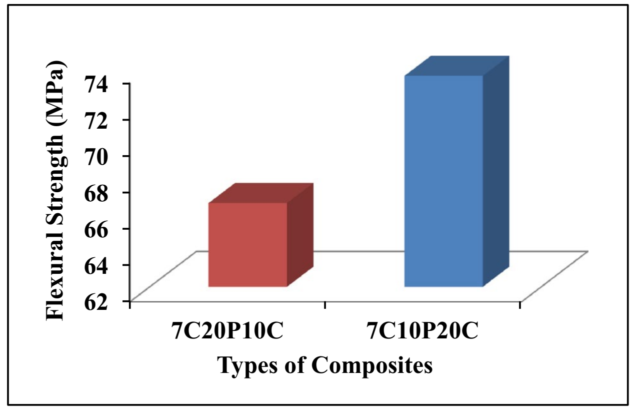

Fig. 5 Flexural strength of CPFLSF/PPLSF hybrid–reinforced composites

the amount of PPLSF is increased, better bonding between the matrix and reinforcement occurs to transfer the load to the PPLSF [14]. In the hybrid reinforced composite, it is observed a considerable reduction in the breaking elongation. The reason was the microcracks are induced at fiber ends due to the high-stress concentration and because of the better interfacial strength between the matrix and PPLSF. Consequently, increasing PPLSF initiated the reduction in breaking elongation values in the hybrid composite.

3.2 Flexural properties

Figures 5 and 6 show the hybridization of CPFLSF with PPLSF leading to the enhancement in the flexural properties of the composites. As the PPLSF weight ratio is increased, the flexural strength also increased considerably. Based on the law of mixture phenomena, increasing the quantity of fiber with high mechanical properties, the bending strength increases linearly. Compared to non-hybrid PPLSF, the flexural strength of the 7C10P20C increased by 3% (73.56MPa). On other hand, associated with non-hybrid PPLSF, the flexural strength of 7C320P10 hybrid–reinforced composite decreased by 6.68%. While the flexural strength of the 7C20P10C hybrid composite was 66.58 MPa, the 7C10P20C strength was 73.56 MPa and 7C10P20C increased by 9.48% compared with that of 7C10P20C.

In terms of the flexural modulus, a similar tendency to the flexural strength was observed. The non-hybrid PPLSF and CPFLSF composites showed the maximum and lowest flexural modulus compared to the hybrid reinforced composites. In comparison with the non-hybrid PPLSF–based composites, the 7C10P20 hybrid composites had shown a significant improvement in the flexural modulus. The flexural modulus of 7C10P20C is 4.98 GPa, and for the hybrid composites, it increased by 3% compared to non-hybrid PPLSF–based composites. Increasing the CPFLSF content in the hybrid composites resulted in the flexural modulus of 4.07 GPa and it led to the decrease in the flexural modulus of 15.3% compared to non-hybrid PPLSF–based composites. Furthermore, the 7C10P20C had revealed the highest improvement up to 18% in the flexural modulus when compared to the 7C20P10C.

As stated before, the extreme weight ratio of PPLSF led to an increase in mechanical properties. Instead, the intention why PPLSF increases bending resistance more efficiently than CPFLSF is that PPLSF has good mechanical properties than CPFLSF. Apart from all contexts, the fiber-matrix interfacial adhesion, types of fiber, and weight ratio are accountable for increasing the flexural properties of the hybrid composite [10].

3.3 Impact properties

The Charpy impact test was done to attain the impact strength of CPFLSF/PPLSF hybrid–reinforced composites

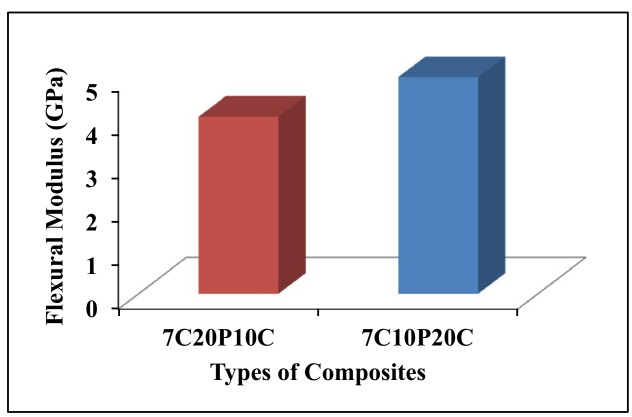

Fig. 6 Flexural modulus of CPFLSF/PPLSF hybrid–reinforced composites

with several fiber ratios and Fig. 7 illustrates the impact strength of the hybrid reinforced composites. The 7C10P20C had shown the maximum impact strength of 10.21 kJ/m^2 which is increased by 3.314% compared to the non-hybrid PPLSF–reinforced composites (10.21kJ/m^2). On the other hand, the non-hybrid CPFLSF–reinforced composite had illustrated the impact strength was 8.25 kJ/m^2. The impact strength of 7C10P20C increased by 21.25%. However, the 7C10P20C has shown the highest impact strength of 10.56 kJ/m^2, when compared to the 7C20P10C, the impact strength higher by 7.88%.

In the hybrid reinforced composite, the energy absorption and impact strength were considerably improved for an increase in the PPLSF weight ratio due to the maximum cellulose content, which provides the higher strength to the PPLSF. Based on the results obtained from the hybrid composite, the impact properties are highly dependent upon the fiber-matrix interfacial bonding characteristics. Table 3 shows the comparison between the mechanical properties of the hybrid CPFLSF/PPLSF–reinforced composites with other short natural fiber hybrid composites [2].

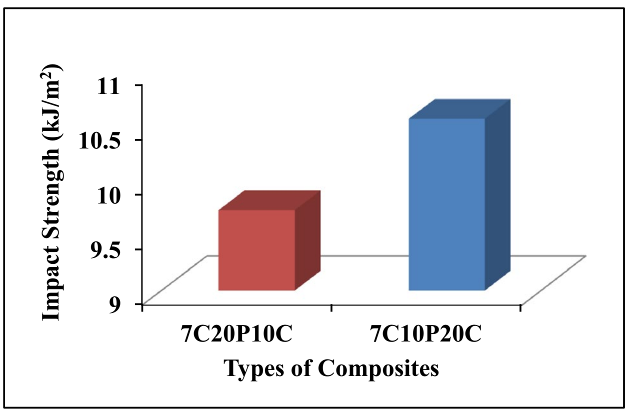

Fig. 7 Impact strength of CPFLSF/PPLSF hybrid–reinforced composites

Although the mechanical properties of the fibers listed in Table 3, the 7ATC10P20C sample exceeds the other natural fiber composites. The low-cost, lightweight, bio-based polyester composites have gained more attention due to their renewability and biodegradability. Moreover, 7ATC10P20C has shown that the mechanical properties of the natural fiber composites are similar or even better than the CPFLSF, jute, straw, sisal, banana, coir, hemp, and kenaf fiber–reinforced composites. Natural fibers have other advantages such as availability, low cost, good thermal and acoustic insulation properties, energy recovery, reduced tool wear in processing operations, degradability, and irritation of the respiratory tract.

However, another important observation is that natural fiber–reinforced composites (CPFLSF and PPLSF) are reported to be more expensive than other synthetic fibers and have the same mechanical properties. Therefore, selecting the most suitable natural fiber for a specific application requires a thorough analysis followed by a decision-making process. Despite all these problems, there are still several markets and industries that have interesting applications for natural fibers.

3.4 Density and void fraction analysis

Table 4 illustrates the theoretical and actual density and void fraction of hybrid composites for different weight percentages. The predicted density was higher than the measured density, as can be shown in Table 3. This can be due to the pores and spaces that were created during the manufacture of the composite.

Table 3 Mechanical properties of 7ATPPLSFC and 7ATCPFLSFC with different natural fiber composites

Composite	Tensile strength (MPa)	Tensile modulus (GPa)	Flexural strength (MPa)	Flexural modulus (GPa)	Impact strength (kJ/m^2)
7ATC10P20C (present work)	47.14±1.743	2.67±0.121	73.56±2.05	4.98±0.219	10.56±0.565
PPLSF	36.13	2.13	71.35	4.81	10.21
CPFLSF	34.31	1.81	58.43	3.23	8.25
Jute	34.78	1.88	66.25	3.69	8.67
Straw	32.67	1.62	47.10	2.17	2.65
Sisal	28.55	1.49	53.42	4.25	9.61
Banana	17.69	1.03	33.51	1.59	9.36
Coir	18.61	1.16	31.15	1.50	3.91
Hemp	34.63	2.56	60.51	3.47	7.36
Kenaf	32.14	2.48	57.35	2.99	3.24
Ramie	32.66	1.58	55.64	3.89	9.32

Table 4 Theoretical and actual density and void fraction of hybrid composites

Composite	Theoretical density (gm/cc)	Measured density (gm/cc)	Volume fraction of voids (%)
7C20P10C	1.093	1.081	1.097
7C10P20C	1.099	1.075	2.183

Table 5 Weight of the hybrid composite for every 30 min

Time period (minutes)	7C20P10C	7C10P20C
30	2.418	2.442
60	2.438	2.444
90	2.447	2.452
120	2.46	2.471
150	2.467	2.479
180	2.49	2.484

3.5 Water absorption properties

The water uptake of the hybrid CPFLSF/PPLSF–reinforced composites with two comparative fiber weight ratios was determined. Even though, the wetting property of materials is purely based on the chemical treatment of the fiber and moisture sensitivity of the material. Tables 5 and 6 show that 7C10P20C hybrid composites significantly have reduced moisture uptake, compared to the 7C20P10C. Figures 8 and 9 show the moisture uptake percentage of the hybrid reinforced composites with immersion time. Based on the plotted curve, the water absorption uptake percentage is increased with the increase of soaking time in the case of the hybrid reinforced composite. Compared to the water absorption uptake properties of the non-hybrid PPLSF composite, the 7C10P20C increased linearly but significant change only was observed [21]. 7C20P10C composites the water absorption uptake properties increased linearly and a fast diffusion rate of water into the composites occurred, which was observed in an increase in water absorption percentage. However, the water diffusion into the composites saturated once the saturation point was reached. It is concluded that the water absorption properties of CPFLSF/PPLSF-reinforced hybrid are comparatively less [18].

3.6 Dynamic mechanical analysis (DMA)

3.6.1 Storage modulus (E′)

Figure 10 shows the storage modulus of the two types of hybrid reinforced composite made of CPFLSF/PPLSF such as 7C20P10Cand 7C10P20C. The results illustrate that, initially, the storage modulus (E′) values are maximum for both

Table 6 Weight percentage of the hybrid composite for every 30 min

Time period (minutes)	7C20P10C	7C10P20C
30	3.253907	1.252177
60	4.107951	1.335102
90	4.492271	1.666805
120	5.047399	2.454598
150	5.346315	2.786301
180	6.328465	2.993615

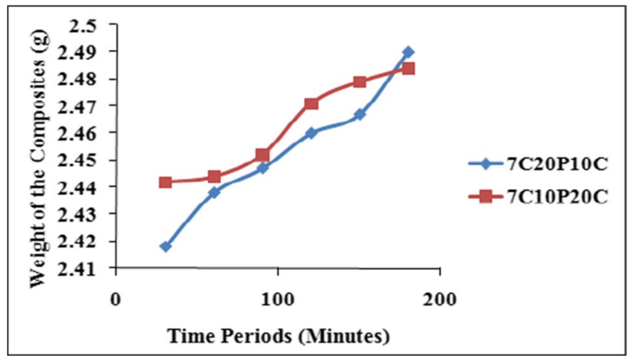

Fig. 8 Water absorption weight of 7C20P10C and 7C10P20C for every 30 min

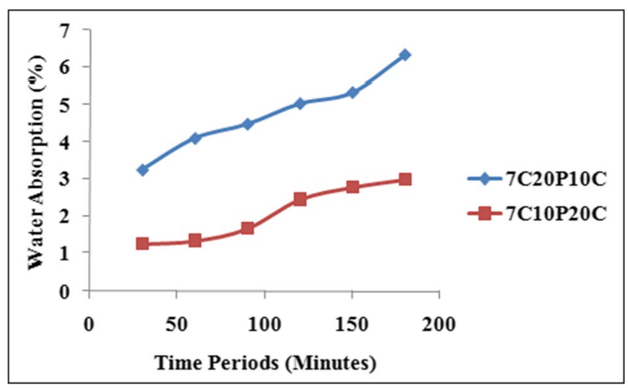

Fig. 9 Water absorption weight percentage of 7C20P10C and 7C10P20C for every 30 min

the hybrid reinforced composites. Furthermore, increasing the temperature gradually, the storage modulus (E′) value is observed to be reducing. When compared with non-hybrid reinforced composite, the storage modulus (E′) exhibits almost the same behavior as the non-hybrid reinforced composites with increasing temperature. Moreover, a significantly maximum storage value (E′) of 1392MPa is obtained for the 7C10P20 hybrid composite, due to the better effect of fiber on the cross-linking to transferring stress [22]. PPLSF had a rough structure along the surface of the fiber due to the chemical treatment and hydrophobic ability which rises interlocking between reinforcement and matrix providing better stress transfer between them [11]. Much less energy is stored since the CPFLSF fiber can move with the force giving a rapid decline in storage modulus [23].

3.6.2 Loss modulus (E″)

Figure 11 shows the variation in the loss modulus (E″) for an increase in temperature for the 7C20P10C and 7C10P20C. The 7C20P10C and 7C10P20C had a peak value of 259.2 MPa and 231.4 MPa in the temperature range of 60 to 200°C. The maximum loss modulus was absorbed for the 7C10P20C, because of energy dissipation as per the heat cycle under the deformation practiced in viscoelastic material. The loss modulus graphs expose that the hybrid composites with PPLSF lead to an increase in the modulus peak [4].

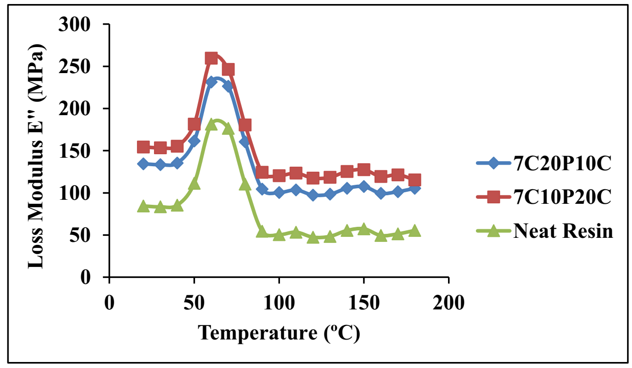

Fig. 11 Loss modulus of CPFLSF/PPLSF hybrid–reinforced composites

3.7 Damping factor (tanδ)

Damping factor (tanδ) can be related to the impact resistance of a composite material. Figure 12 illustrates the damping factor (tanδ), and characteristics of 7C20P10C and 7C10P20C. From the curve, the 7C10P20C showed the lower peak value of damping factor = 0.184, which indicates the good interfacial bonding between the matrix and fiber due to the chemical treatment of the fiber. Comparing both the hybrid composites, the damping factor value is found to change significantly. However, the higher peak value of the damping factor provides poor interfacial bonding between the matrix and fiber [6].

3.8 Thermogravimetric analysis of composite

The thermal decomposition for PPLSF/CPFLSF-reinforced composites is shown in Figs. 13 and 14. From the observation of TGA, the 7C20P10C and 7C10P20C had three-stage decomposition. The initial decomposition was at 100 to 250°C, which was related to the degradation of water and other volatile mixtures in the hybrid reinforced composite. Then, the second stage of decomposition was at 300 to 450°C. In this region, the thermal degradation happened due to the decomposition of hemicelluloses and lignin of PPLSF/CPFLSF. The final thermal decomposition stage of 7C20P10C and 7C10P20C happened in the temperature range between 500 and 600°C, with residual content of 18% and 26%. Because of the thermal decomposition of cellulose and end with the decomposition matrix [16].

The peak region of the DTA curves specifies the degradation temperatures of the 7C20P10C and 7C10P20C. From the DTA curves, the peak region for 7C20P10C and 7C10P20C is at 415 °C and 425°C, which displayed stages of degradation in the composite with the highest rate of decomposition at 1.2%/min and 1.4%/min, respectively. Compared to the non-hybrid PPLSF composite, the DTA of the hybrid composite is significantly improved at the end temperatures as shown in Fig. 14.

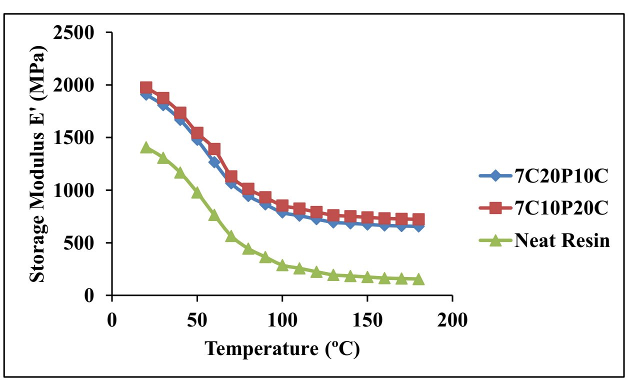

Fig. 10 Storage modulus of CPFLSF/PPLSF hybrid–reinforced composites

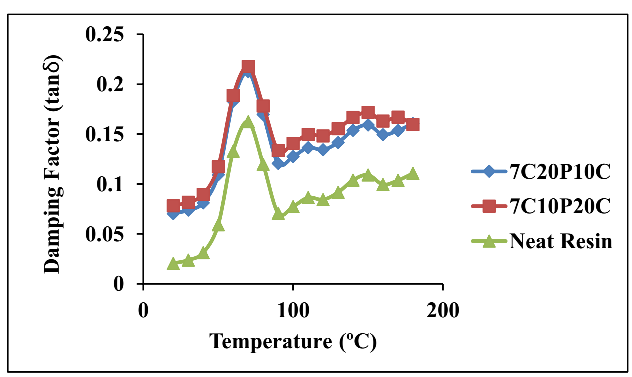

Fig. 12 Damping factor of CPFLSF PPLSF hybrid–reinforced composites

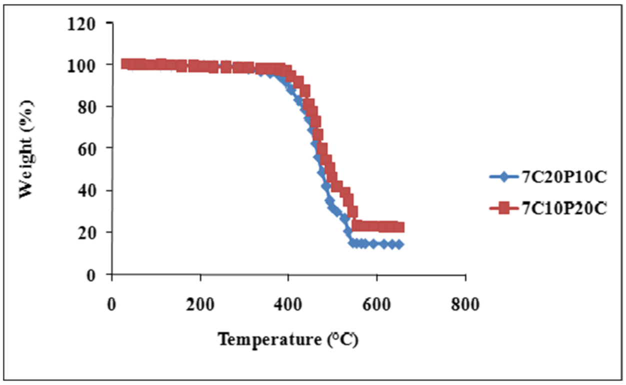

Fig. 13 Thermogravimetric analysis curve of CPFLSF/PPLSF hybrid–reinforced composites

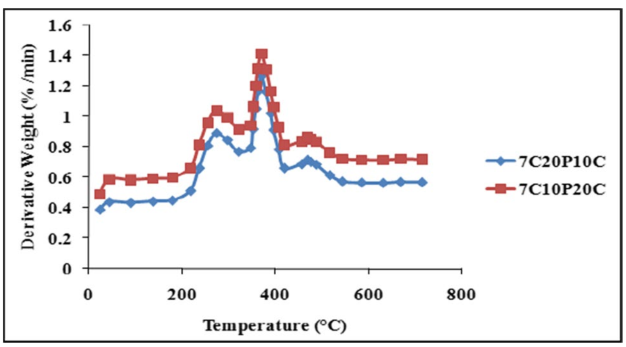

Fig. 14 Differential thermogravimetric analysis curve of CPFLSF/PPLSF hybrid–reinforced composites

3.9 Scanning electron microscope

Figure 15(a–b) show the SEM of tensile fractured surfaces of the 7C20P10C and 7C10P20C. Poor adhesion between the fiber and matrix as well as matrix cracks was observed in the 7C20P10C due to the maximum weight ratio of CPFLSF. However, 7C20P10C the failure had occurred due to fiber tearing and the CPFLSF pullout from the matrix (Fig. 15(a)) [19]. The alkali treatment increased fiber-matrix adhesion and also reduced fiber pullouts resulting in increased mechanical properties of the 7C10P20C (Fig. 15(b)). In the 7C10P20C, PPLSF had maximum tensile properties and provide a better stress transfer compared to7C20P10C.

In hybrid composite material, the load was carried by CPFLSF; then, it was transferred to PPLSF without affecting the matrix in the tensile specimen [24]. The highest strain rate is attained by CPFLSF, so the failures occur in the CPFLSF; after that, PPLSF took the load and effectively transferred the load, which enhances the properties of 7C10P20C [19].

4 Conclusions

The alkali-treated randomly distributed CPFLSF/PPLSF-reinforced polyester hybrid composites were fabricated and investigated for static, dynamic mechanical, thermal, and water absorption properties. From this research work, the following conclusions are arrived.

1. The randomly distributed alkali-treated CPFLSF/PPLSF–reinforced hybrid composites showed that the 7C10P20C exhibited the maximum tensile strength of 47.14MPa, flexural strength of 73.56MPa, and impact strength of 10.56kJ/m^2. The SEM analysis also confirmed the evidence of less pullout and fracture. The improvement in strength is due to the presence of the palmyra palm leaf stalk fiber in the hybrid composites.
2. The dynamic mechanical analysis of CPFLSF/PPLSF–reinforced hybrid composites showed that the 7C10P20C exhibited the maximum storage modulus (E′) of 1975MPa and loss modulus (E″) of 251.4MPa and low damping factor (tanδ) of 0.21.

Fig. 15 SEM image of tensile test fractured composite surfaces of **a** 7C20P10C and **b** 7C10P20C

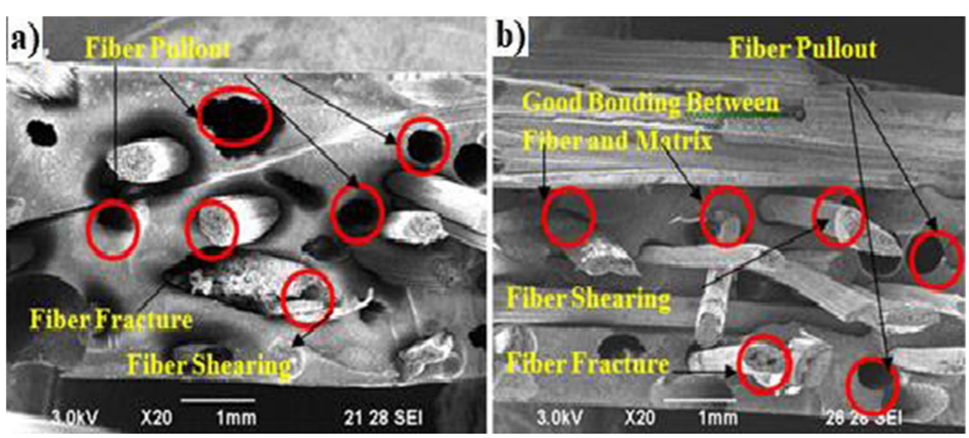

3. Water absorption was found to significantly reduce in 7C10P20C compared to the 7C20P10C.
4. 7C20P10C and 7C10P20C exhibited thermal decomposition in the temperature range between 500 and 600°C with a residual mass of 18% and 26%, respectively. Due to its comparable behavior to synthetic fiber composites, hybrid reinforced composites have a wide range of potential uses.

Author contribution Dr. Rama Thirumurugan and Dr. Jayaraj Mahalingam conceived the presented idea. Dr. Jayaraj Mahalingam developed the composite of materials. Dr. D. Shanmugam and Dr. Jayaraj Mahalingam verified the analytical methods and test results. Dr. Rama Thirumurugan encouraged Dr. D. Shanmugam to investigate and supervised the findings of this work. All authors discussed the results and contributed to the final manuscript.

Declarations

Ethics approval Not applicable

Conflict of interests The authors declare no competing interests.

References

1. Saheb DN, Jog JP (1999) Natural fiber polymer composites: a review. Adv Polym Technol: J Polym Proc Inst 18(4):351–363. https://doi.org/10.1002/(SICI)1098-2329(199924)18:4%3c351::AID-ADV6%3e3.0.CO;2-X
2. Gurunathan T, Mohanty S, Nayak SK (2015) A review of the recent developments in biocomposites based on natural fibres and their application perspectives. Compos A: Appl Sci Manuf 77:1–25. https://doi.org/10.1016/j.compositesa.2015.06.007
3. Satyanarayana KG, Arizaga GG, Wypych F (2009) Biodegradable composites based on lignocellulosic fibers—an overview. Prog Polym Sci 34(9):982–1021. https://doi.org/10.1016/j.progpolymsci.2008.12.002
4. Zhang MQ, Rong MZ, Lu X (2005) Fully biodegradable natural fiber composites from renewable resources: all-plant fiber composites. Compos Sci Technol 65(15–16):2514–2525. https://doi.org/10.1016/j.compscitech.2005.06.018
5. Dahy H (2019) Natural fibre-reinforced polymer composites (NFRP) fabricated from lignocellulosic fibres for future sustainable architectural applications, case studies: segmented-shell construction, acoustic panels, and furniture. Sensors 19(3):738. https://doi.org/10.3390/s19030738
6. Eslahi N, Mahmoodi A, Mahmoudi N, Zandi N, Simchi A (2020) Processing and properties of nanofibrous bacterial cellulose-containing polymer composites: a review of recent advances for biomedical applications. Polym Rev 60(1):144–170. https://doi.org/10.1080/15583724.2019.1663210
7. Satyanarayana KG, Pillai CKS, Sukumaran K, Pillai SGK, Rohatgi PK, Vijayan K (1982) Structure property studies of fibres from various parts of the coconut tree. J Mater Sci 17(8):2453–2462. https://doi.org/10.1007/BF00543759
8. Prades A, Assa RRA, Dornier M, Pain JP, Boulanger R (2012) Characterisation of the volatile profile of coconut water from five varieties using an optimised HS-SPME-GC analysis. J Sci Food Agr 92(12):2471–2478. https://doi.org/10.1002/jsfa.5655
9. Muruganrama, Thiru, Jayaraj Mahalingam, Shanmugam Dharmalingam, and Shanmugasundaram Natarajan (2022) Investigation of static and dynamic mechanical properties of short palmyra palm leaf stalk fiber (PPLSF) reinforced polymer composites. J Nat Fibers 19:1908–1924. https://doi.org/10.1080/15440478.2020.1840478.
10. Prasath SA, Balamurugan V, Ganesh SS, Murthy AU (2018) Evaluation of mechanical properties on banyan fiber reinforced polymer matrix composite using FEA. In IOP Conf Ser: Mater Sci Eng (Vol. 402, No. 1, p. 012135). IOP Publishing. https://doi.org/10.1088/1757-899X/402/1/012135
11. Manimaran P, Senthamaraikannan P, Sanjay MR, Marichelvam MK, Jawaid M (2018) Study on characterization of Furcraea foetida new natural fiber as composite reinforcement for lightweight applications. Carbohydr Polym 181:650–658. https://doi.org/10.1016/j.carbpol.2017.11.099
12. de Andrade Silva F, Chawla N, de Toledo Filho RD (2008) Tensile behavior of high performance natural (sisal) fibers. Compos Sci Technol 68(15–16):3438–3443. https://doi.org/10.1016/j.compscitech.2008.10.001
13. Prasad, Lalta, Vinod Singh, Raj Vardhan Patel, Anshul Yadav, Virendra Kumar, and Jerzy Winczek (2021) Physical and mechanical properties of rambans (agave) fiber reinforced with polyester composite materials." J Nat Fibers 1–15. https://doi.org/10.1080/15440478.2021.1904481
14. Prasad L, Bairwan R, Yadav A, Kumar A, Kumar V, Winczek J (2022) Evaluation of physical, mechanical, and wear properties of Jatropha shell powder reinforced epoxy glass fiber composites J Nat Fibers 1–13. https://doi.org/10.1080/15440478.2022.2054892
15. Negi RS, Prasad L, Yadav A, Winczek J (2022) Physical and mechanical properties of pinecone scale fiber/Vigna mungo powder reinforced polypropylene based hybrid composites J Nat Fibers 1–11. https://doi.org/10.1080/15440478.2022.2025983
16. Kumar S, Prasad L, Patel VK, Kumain A, Yadav A (2022) Experimental and numerical study on physico-mechanical properties and Taguchi's designed abrasive wear behavior of hemp/nettle-polyester hybrid composite. Polym Compos 42(12):6912–6927. https://doi.org/10.1002/pc.26350
17. Mulinari DR, Baptista CARP, Souza JVC, Voorwald HJC (2011) Mechanical properties of coconut fibers reinforced polyester composites. Procedia Eng 10:2074–2079. https://doi.org/10.1016/j.proeng.2011.04.343
18. Belouadah, Zouheyr, Mansour Rokbi, and Abdelaziz Ati (2022) Manufacturing and characterization of new composite based on epoxy resin and Lygeum Spartum L. plant. Journal of Natural Fibers 19 : 4236–4248. https://doi.org/10.1080/15440478.2020.1856273
19. Bisanda ETN, Ansell MP (1992) Properties of sisal-CNSL composites. J Mater Sci 27(6):1690–1700. https://doi.org/10.1007/BF00542934
20. Bhuvaneshwaran M, Subramani SP, Palaniappan SK, Pal SK, Balu S (2021) Natural cellulosic fiber from Coccinia indica stem for polymer composites: extraction and characterization. J Nat Fibers 18(5):644–652. https://doi.org/10.1080/15440478.2019.1642826
21. Thirumurugan R, Jayaraj M, Shanmugam D, Ramkumar T (2021) Characterization of new natural cellulosic fiber from coconut tree primary flower leaf stalk fiber (CPFLSF). J Nat Fibers 18(11):1844–1856. https://doi.org/10.1080/15440478.2019.1701608
22. Kumar SS, Duraibabu DA, Subramanian K (2014) Studies on mechanical, thermal and dynamic mechanical properties of untreated (raw) and treated coconut sheath fiber reinforced epoxy composites. Mater Des 59:63–69. https://doi.org/10.1016/j.matdes.2014.02.013

23. Venkataswamy MA, Pillai CKS, Prasad VS, Satyanarayana KG (1987) Effect of weathering on the mechanical properties of midribs of coconut leaves. J Mater Sci 22(9):3167–3172. https://doi.org/10.1007/BF01161178
24. Kumar S, Prasad L, Patel VK, Kumar V, Kumar A, Yadav A (2021) Physico-mechanical properties and Taguchi optimized abrasive wear of alkali treated and fly ash reinforced Himalayan agave fiber polyester composite. J Nat Fibers 1–14. https://doi.org/10.1080/15440478.2021.1982818

Publisher's note Springer Nature remains neutral with regard to jurisdictional claims in published maps and institutional affiliations.